THE JOURNAL OF BIOLOGICAL CHEMISTRY VOL. 286, NO. 2, pp. 1227–1236, January 14, 2011

Dematin, a Component of the Erythrocyte Membrane Skeleton, Is Internalized by the Malaria Parasite and Associates with *Plasmodium* 14-3-3*[S]

Received for publication, October 14, 2010, and in revised form, November 15, 2010 Published, JBC Papers in Press, November 17, 2010, DOI 10.1074/jbc.M110.194613

Marco Lalle[‡], Chiara Currà[‡], Fabio Ciccarone[‡], Tomasino Pace[‡], Serena Cecchetti[§], Luca Fantozzi[‡], Bernhard Ay[¶], Catherine Braun Breton[‖], and Marta Ponzi[‡1]

From the [‡]Dipartimento di Malattie Infettive, Parassitarie ed Immunomediate and [§]Dipartimento di Biologia Cellulare e Neuroscienze, Istituto Superiore di Sanità, 00161 Rome, Italy, the [¶]Institute of Medical Immunology, Charité-Universitätsmedizin Berlin, 10115 Berlin, Germany, and the [‖]Dynamique des Interactions Membranaires Normales et Pathologiques, University Montpellier II, 34095 Montpellier, France

The malaria parasite invades the terminally differentiated erythrocytes, where it grows and multiplies surrounded by a parasitophorous vacuole. *Plasmodium* blood stages translocate newly synthesized proteins outside the parasitophorous vacuole and direct them to various erythrocyte compartments, including the cytoskeleton and the plasma membrane. Here, we show that the remodeling of the host cell directed by the parasite also includes the recruitment of dematin, an actin-binding protein of the erythrocyte membrane skeleton and its repositioning to the parasite. Internalized dematin was found associated with *Plasmodium* 14-3-3, which belongs to a family of conserved multitask molecules. We also show that, *in vitro*, the dematin-14-3-3 interaction is strictly dependent on phosphorylation of dematin at Ser^{124} and Ser^{333}, belonging to two 14-3-3 putative binding motifs. This study is the first report showing that a component of the erythrocyte spectrin-based membrane skeleton is recruited by the malaria parasite following erythrocyte infection.

The *Plasmodium* parasite, the etiologic agent of malaria, invades the host red blood cell (RBC),[2] where it grows and multiplies within a parasitophorous vacuole (PV). The PV membrane (PVM) represents an interface between the parasite and the host erythrocyte. A subset of parasite proteins is exported beyond the PVM by a recently discovered secretory system directed by a pentameric amino acid sequence motif (PE*X*E(L/H)T) (1, 2). Additional pathways might flank this unusual export machinery because a number of parasite proteins that do not contain the PE*X*E(L/H)T motif are also exported to erythrocyte sites (3). The parasite generates novel membrane compartments to sustain protein trafficking. For example, in *Plasmodium falciparum*-infected RBCs (iRBCs), the so-called Maurer's clefts, organelles anchored to the RBC cytoskeleton, are responsible for the assembly and targeting of parasite adhesive proteins to the erythrocyte surface. Exported proteins are routed to different erythrocyte compartments, including the host membrane skeleton, leading to extensive remodeling of the host cell.

The erythrocyte skeleton is anchored to the phospholipid bilayer through two major protein bridges; one connects the integral membrane protein band 3 to spectrin via ankyrin, whereas the other involves the junctional complex, which connects the C-terminal end of spectrin to short actin protofilaments (4, 5). Protein 4.1, dematin, and adducin are components of the junctional complex. Protein 4.1, p55, and the transmembrane glycophorin C form a well characterized ternary complex, which tethers the junctional complex to the plasma membrane (6). The membrane receptors glucose transporter-1 GLUT1 (7) and Band 3 (8) directly bind to dematin and/or adducin, providing alternative links to the erythrocyte plasma membrane.

Several *P. falciparum* exported proteins bring about coordinated remodeling of the spectrin-based erythrocyte membrane skeleton (3, 9). One of the best characterized examples is the knob-associated histidine-rich protein (KAHRP), which is a major component of knobs, conical protrusions on the cytoplasmic side of the host plasma membrane. Multimeric clusters of knob-associated histidine-rich protein associate with spectrin and actin and function as attachment points in cytoadherence. Three exported parasite proteins, the Pf332 protein, the mature parasite-infected erythrocyte surface antigen (MESA), and the erythrocyte membrane protein 3 (PfEMP3), interact with the erythrocyte skeleton and contribute to increase its rigidity. Moreover, a recent reverse genetic screen identified additional proteins, which influence erythrocyte deformability, most probably acting directly or indirectly on the erythrocyte cytoskeleton (9).

Here, we show that the host skeletal protein dematin is translocated within the parasite, where it interacts with the *Plasmodium* 14-3-3 isoform (10, 11). 14-3-3 proteins belong to a family of highly conserved molecules present in virtually all eukaryotes as single or multiple isoforms (12). They exist

* This work was supported by grants from the European Commission Seventh Framework Programme (FP7/2007-2013) under Grant Agreement 242095.

[S] The on-line version of this article (available at http://www.jbc.org) contains supplemental Experimental Procedures, Tables S1 and S2, and Figs. S1–S3.

[1] To whom correspondence should be addressed: Dipartimento di Malattie Infettive, Parassitarie ed Immunomediate, Istituto Superiore di Sanità, Viale Regina Elena 299, 00161 Roma, Italy. Tel.: 39-0649902868; Fax: 39-0649902226; E-mail: marta.ponzi@iss.it.

[2] The abbreviations used are: RBC, red blood cell; iRBC, infected RBC; PV, parasitophorous vacuole; PVM, parasitophorous vacuole membrane; Ab, antibody; CLSM, confocal laser scanning microscopy; PK, proteinase K.

as homo- and/or heterodimers and function as versatile proteins routed from the cytosol to different cellular organelles and membrane compartments. 14-3-3 proteins are able to bind a broad range of Ser/Thr-phosphorylated target proteins and are thus involved in a large number of cellular processes.

EXPERIMENTAL PROCEDURES

Parasite Cultivation and Manipulation—The murine *Plasmodium berghei* ANKA, clone 8417HP, was used for all the analyses. Asynchronous infections were established in CD1 mice by intraperitoneal injection of infected blood. Blood was collected by heart puncture under anesthesia, and leukocytes were removed using Plasmodipur leukocyte filters (Euro-Diagnostica, Malmö, Sweden). *P. berghei* synchronous infections, parasite purification, and transfection were performed as described (13, 14). Asexual stages of *P. falciparum* 3D7 line were cultured and synchronized by standard procedures (15).

Vectors—Vector construction and primers are detailed in the supplemental Experimental Procedures and supplemental Table 1. The transfection vector Pb14-3-3/def containing a FLAG-tagged copy of the *P. berghei* 14-3-3 was linearized with SmaI and introduced into merozoites of *P. berghei* to produce the transgenic line *FLAG*_Pb14-3-3. The plasmid pQE30::Pb14-3-3 contains the Pb14-3-3 coding sequence fused with the hexahistidine tag. The plasmid pGEX6P1::dematin52 contains the coding sequence of the 52-kDa isoform of mouse dematin. The plasmids pGEX6P1::S403A, pGEX6P1::S124A, pGEX6P1::S124A/S403A, pGEX6P1::S333A/S403A, and pGEX6P1::S124A/S333A/S403A contain dematin with single, double, or triple mutations of serines 124, 403, and 333 into alanines. The plasmid pDIF-X, for the expression of GST-fused difopein, was previously described (16). PCR reactions were performed using 20 pmol of each primer and 1.25 units of Ex Taq (Takara Holdings Inc.). Amplification conditions were: 1 cycle at 95 °C for 5 min; 30 cycles at 95 °C for 30 s, 55 °C for 30 s, and 72 °C for 30 s; and 1 cycle at 72 °C for 7 min.

Expression and Purification of the Recombinant Proteins—*Escherichia coli* strains expressing the GST or the His fusions were induced with 0.5 mM isopropyl-1-thio-β-D-galactopyranoside. GST-tagged proteins were purified by affinity chromatography on glutathione-Sepharose 4B (GE Healthcare). Elution was performed with 10 mM reduced glutathione, pH 8.0. When required, proteins were released from the GST by digestion with the PreScission protease (GE Healthcare) following the manufacturer's instructions.

Immune Sera—50 μg of purified GST-released recombinant Pb14-3-3 or 52-kDa dematin, in complete Freund's adjuvant, were injected intraperitoneally in Balb/c mice. The immunization procedure was repeated using 25 μg of recombinant protein in incomplete Freund's adjuvant after 28, 42, 56, and 70 days from the first inoculum. At day 84, immunized mice were bled to obtain the immune sera α-Pb14-3-3 and α-52-kDa-dematin (md52k). Prior to immunization, blood was collected from the submandibular vein of each mouse to obtain preimmune sera.

P. berghei Protein Extracts—Parasites (2×10^9) surrounded by the parasitophorous vacuole (vacuolar parasites) were purified as described (10) and frozen at −80 °C. All buffers used were supplemented with the protease inhibitor P8340 (Sigma-Aldrich) and phosphatase inhibitor mixtures P2850 (Sigma-Aldrich). Protein concentration was measured (Bradford solution, Pierce). Centrifugations were performed at 24,000 × *g* for 30 min at 4 °C. Parasites were resuspended in 2 volumes of extraction buffer (30 mM Tris-HCl, 1 mM DTT, and 1 mM EDTA, pH 7.4) and sonicated five times for 30 s at 60% power and 10% duty cycle) with a Sonoplus ultrasonic homogenizer (Bandelin Electronic, Berlin, Germany). The lysate was centrifuged, and the supernatant was collected. Sediment, containing the insoluble material, was washed twice with cold PBS and centrifuged. Alternatively, vacuolar parasites were resuspended with 200 μl of cold PBS and disrupted by five cycles of freezing in liquid nitrogen and thawing at 37 °C. The soluble fraction was collected by centrifugation. The pellet was washed with cold PBS and incubated with 100 μl of high salt extraction buffer (20 mM HEPES, pH 7.8, 800 mM KCl, 1 mM EDTA, 1 mM DTT) for 30 min at 4 °C. After centrifugation, the collected supernatant (high salt soluble fraction) was diluted with 100 μl of dilution buffer (20 mM HEPES, pH 7.8, 1 mM EDTA, 1 mM DTT). The pellet was washed with high salt extraction buffer, centrifuged, and solubilized with 2× Laemmli sample buffer.

Total lysate of *Toxoplasma gondii* tachyzoites of the strains RH (gift of Furio Spano) was obtained by incubating parasites in radioimmune precipitation buffer (150 mM NaCl, 1% Nonidet P-40, 0.5% sodium deoxycholate, 0.1% SDS, 50 mM Tris-HCl, pH 8.0) for 20 min in ice. Total lysate of *Cryptosporidium parvum* sporozoites was prepared from 8×10^7 excysted oocysts (gift of Fabio Tosini) obtained from experimentally infected calves, as described previously (17). Human and mouse red blood cell ghost proteins were prepared as described previously (18).

Western Blot Analysis and Overlay Assay—Procedures were detailed in the supplemental Experimental Procedures. Antibodies used were: mouse α-FLAG monoclonal antibody (mAb) (Sigma-Aldrich), 1:1000; mouse α-Pb14-3-3 serum, 1:2000; mouse α-Hu14-3-3 serum (Ab14110, Abcam plc, Cambridge, UK) against the full-length Hu14-3-3γ, 1:500; rabbit α-Pan-14-3-3 serum (Ab14112; Abcam), against the conserved N-terminal peptide KAKLAEQAER of human β isoform, 1:500; mouse α-dematin mAb (611062, BD Transduction Laboratories), against the dematin region encompassing residues 68–190, 1:2000; mouse md52kd, 1:1000; goat α-GST mAb HRP-conjugated (GE Healthcare), 1:2000; mouse α-His_6 mAb (Sigma-Aldrich), 1:1000; mouse anti-BR5, against the N terminus of the Pfsbp1 protein, 1:1000; and mouse α-pfHsp70 serum (19), 1:1000. The overlay assay was performed as described previously (16) using 5 μg/ml GST-Pb14-3-3 as a bait.

Peptide Array Synthesis—The procedure to prepare membrane-bound peptides covering the *P. berghei* 14-3-3 is detailed in the supplemental Experimental Procedures and supplemental Fig. S1. Peptides are listed in supplemental Table S2.

Immunofluorescence Assay—*P. berghei* or *P. falciparum*-infected erythrocytes were fixed (4% EM-grade paraformaldehyde, 0.0075% EM-grade glutaraldehyde in PBS) for 30 min at room temperature, permeabilized (0.1% Triton X-100 in PBS)

for 10 min, and layered onto slides. Parasites were blocked with 1% gelatin in PBS for 30 min and incubated with the primary antibody for 1 h at room temperature. After repeated washes with PBS, the slides were incubated with the fluorochrome-conjugated secondary antibody 1:200 (Invitrogen) for 30 min at room temperature. After washes with PBS, the slides were mounted with the anti-fading agent VECTASHIELD (Vector Laboratories, Burlingame, CA) supplemented with 300 nM 4′,6-diamidino-2-phenylindole (DAPI) to stain parasite nuclei. The following antibodies were used: rabbit α-PbSEP1 (20), 1:100; rabbit α-EXP1 (21), 1:100; rabbit α-Pan14-3-3, 1:30; mouse α-dematin mAb, 1:30; mouse md52kd, 1:100; and mouse α-Pb14-3-3, 1:100. Primary antibodies were revealed with either Alexa Fluor 488-conjugated or Alexa Fluor 546-conjugated anti-mouse or anti-rabbit secondary Abs. Confocal laser scanning microscopy (CLSM) observations were performed at room temperature with a Leica TCS SP2 AOBS apparatus, using a 100×/1.40 numeric aperture of the oil objective and the excitation spectral laser lines at 405, 488, and 594 nm, properly tuned by an acousto-optical tunable filter. The emission wavelengths were selected by a proper setting of the spectral detection system. Image acquisition was carried out using the Leica Confocal Software version 2.3 (Leica Lasertechnik, Heidelberg, Germany). Signals from the different fluorescent probes were taken in sequential scan mode, and co-localization was detected in yellow. Image deconvolution was performed using the Huygens software (Scientific Volume Imaging BV, Hilversum, The Netherlands). Different fields of view (>200 cells) were analyzed on the microscope for each labeling condition, and representative results were shown.

Affinity Purification—FLAG-Pb14-3-3 was purified using the mouse α-FLAG mAb covalently bound to agarose beads (Sigma-Aldrich). The column was prepared following the manufacturer's instructions. *P. berghei* mixed blood stages from the parental HP or from the *FLAG*_Pb14-3-3 transgenic line were sonicated to disrupt the parasites, and the soluble fraction was incubated with anti-FLAG beads at 4 °C for 3 h. After washes with 100 resin bed volumes of HT buffer (20 mM Hepes-KOH, pH 7.6, 75 mM KCl, 5 mM $MgCl_2$, 0.1 mM EDTA, 0.04% Tween 20), proteins were eluted with 200 μM synthetic FLAG peptide (Sigma-Aldrich) at 4 °C for 1 h. The collected material was stored at −80 °C until use.

Dematin Immunoprecipitation Assay—Mouse α-dematin mAb (25 μg) was bound and cross-linked to 50 μl of Dynal protein-G magnetic beads (Invitrogen) according to the manufacturer's instructions. The *P. berghei* soluble protein fraction (1 mg), obtained by sonication, was preincubated with 50 μl of Dynal protein-G magnetic beads (Invitrogen) in 1 ml of KHT (HT buffer supplemented with 150 mM KCL) for 1 h at room temperature with gentle shaking. Precleared material was incubated with α-dematin-coupled Dynal protein-G in the same conditions. Beads were washed five times with KHT, and the immunoprecipitated material was recovered in 2× Laemmli sample buffer after heating at 75 °C for 10 min.

Pulldown Assay—*P. berghei* soluble proteins (0.5 mg), obtained by sonication, were incubated for 1 h at 4 °C in HT buffer with 5 μg of glutathione-Sepharose-immobilized GST-Pb14-3-3 to pull down the internalized dematin or with 5 μg of glutathione-Sepharose-immobilized GST-difopein to pull down the Pb14-3-3. Glutathione-Sepharose-immobilized GST was used as a control. After washes with buffer HT, bound proteins were eluted for 1 h at 4 °C with 50 μl of 2 mM A8Ap synthetic phosphopeptide ARAApSAPA, where pS is a phosphoserine (22), reproducing a 14-3-3-binding motif. Aliquots of the eluted material were run in SDS-PAGE and subjected to immunoblotting with the indicated antibodies.

In Vitro Kinase Assay—Recombinant GST-dematin (10 μg), bound to glutathione-Sepharose beads, was placed in 30 μl of cAMP-dependent protein kinase A (PKA) buffer (20 mM Tris-HCl, pH 7.5, 100 mM NaCl, 12 mM $MgCl_2$, 1 mM DTT, 200 μM ATP) with 10 units of porcine PKA catalytic subunit (Sigma-Aldrich) or casein kinase II buffer (20 mM Tris-HCl, pH 7.5, 50 mM KCl, 10 mM $MgCl_2$, 200 μM ATP) with 15 units of casein kinase II (New England Biolabs, Beverly, MA) in the presence of 2.5 μCi of [γ-^{32}P]ATP. Samples were incubated for 1 h at 30 °C, and the reactions were stopped with 5 mM EDTA. After washes with TBS with Tween, recombinant dematin was eluted from the beads with the PreScission protease treatment. Phosphorylated polypeptides were detected by autoradiography of dried gels.

In Vitro Pb14-3-3 Binding Assay—5 μg of glutathione-Sepharose-immobilized GST, GST-dematin, or dematin mutants were phosphorylated with PKA as described and incubated with 0.5 μg of bacterial lysate expressing His-Pb14-3-3, in buffer HT for 1 h at 4 °C. After washes with buffer HT, bound His-Pb14-3-3 was recovered first with 50 μl of 2 mM A8Ap phosphopeptide for 1 h at 4 °C. GST and GST-dematin or dematin mutants were recovered with 10 mM reduced glutathione, pH 8.0. Eluted material was separated by SDS-PAGE and analyzed by Western blot using α-His_6 antibody (Qiagen).

Subcellular Fractionation of iRBC and Proteinase K Digestion Assay—Purified *P. falciparum* iRBCs were incubated for 30 min at 37 °C with streptolysin-O (La Technique Biologique, Paris, France) to permeabilize RBC membrane, leaving intact the PVM (23). Erythrocyte cytoplasm and parasites were separated by low speed centrifugation (2000 × *g* for 10 min at 4 °C). iRBC cytoplasm was successively spun down at high speed (15,000 × *g* for 30 min at 4 °C) to recover ghosts. Parasite pellet and ghosts were extensively washed with PBS. Proteinase K (Roche Diagnostics GmbH, Mannheim, Germany) treatment was performed on purified vacuolar parasites and iRBC ghosts as described (18). Samples were separated by SDS-PAGE and analyzed by Western blot.

RESULTS

Expression and Immunolocalization of P. berghei 14-3-3—Previous immunolocalization studies detected the multifunctional 14-3-3 protein in both human and rodent *Plasmodium* sp. (10, 11). Due to the high degree of similarity shared by eukaryotic 14-3-3 proteins, we decided to determine the tryptic map of the 14-3-3 protein(s) present in the soluble fraction of *P. berghei* mixed blood stages. 14-3-3 was purified, taking advantage of its affinity for a synthetic polypeptide (difopein) containing a tandem repeat of the 14-3-3 phosphorylation-independent binding motif WLDLE (24). MALDI mass spec-

trometry (MS) analysis (supplemental Fig. S1, *A* and *B*) allowed us to unambiguously identify the purified material as the product of the *P. berghei* 14-3-3-encoding gene (PlasmoDB accession number PB000900.00.0). No peptides corresponding to the host 14-3-3 proteins were detected in an exhaustive analysis of the acquired spectra (data not shown).

Plasmodium 14-3-3 is conserved within the genus and shares similarities with the 14-3-3 proteins from other apicomplexan parasites (supplemental Fig. S1*B*). It contains 14-3-3-characteristic structural and functional domains, such as those involved in dimer formation and in target binding (supplemental Fig. S1*B*).

A polyclonal mouse immune serum (α-Pb14-3-3) was prepared using purified recombinant Pb14-3-3-GST fusion protein; the epitopes it reacts with were identified by pepscan analysis. For this purpose, peptides covering the entire Pb14-3-3 protein sequence were synthesized on a cellulose membrane support (supplemental Table S2) and probed with the αPb14-3-3 immune serum (supplemental Fig. S1*C*). Except for the conserved N-terminal peptide LRSDCTYRSKLAEQAERYDEM, the four additional epitopes, recognized by the immune serum, are specific to *Plasmodium* 14-3-3. They are partially conserved in other apicomplexan parasites but completely absent in mammalian isoforms (supplemental Fig. S1*B*). Based on the proposed structural model of the *P. berghei* 14-3-3 (supplemental Fig. S1*D*), these epitopes reside in a variable external region of the protein, outside the target-binding groove (24, 25). In particular, an immunogenic short amino acid stretch, CVNNDKD, present exclusively at the N terminus of the *Plasmodium* 14-3-3, seems to form an extra loop between α helices 2 and 3.

In Western blot analysis (Fig. 1*A*), the αPb14-3-3 polyclonal serum detected a band of the expected apparent molecular weight in protein extracts of *P. berghei*, *P. falciparum*, *T. gondii*, and *C. parvum,* whereas it did not recognize mammalian isoforms present in human or mouse erythrocytes. Thus, despite its reactivity with a conserved N-terminal peptide, the antiserum specifically recognizes only 14-3-3 proteins of parasitic origin. These data confirmed that the αPb14-3-3 antiserum mainly recognized structural features specific to the Apicomplexa. Consistently, antibodies against a conserved N-terminal epitope of the mammalian β isoform (α-pan14-3-3) detected all of the 14-3-3 proteins tested (Fig. 1*A*).

In fractionated parasite extracts, the Pb14-3-3 was mainly detected in the soluble fractions, whereas a minor proportion was associated with insoluble material in both asexual and sexual stages (Fig. 1*B*). Immunolocalization studies (Fig. 1*C*) detected 14-3-3-specific fluorescence exclusively inside the parasite throughout the erythrocyte cycle. This was confirmed (Fig. 1*C*) by double fluorescence, using antibodies against the PVM-resident SEP/ETRAMP family member PbSEP1 (20).

We also generated a *P. berghei* transgenic line *FLAG*_Pb14-3-3 containing a second integrated copy of the Pb14-3-3 fused at the N terminus with a FLAG immuno-tag (FLAG-Pb14-3-3) and driven by the upstream and downstream regulatory regions of the endogenous gene. In immunolocalization experiments, FLAG-specific mAb detected the FLAG-Pb14-3-3 version exclusively inside the parasite, consistent with the subcellular localization of the endogenous protein (supplemental Fig. S2*A*). In Western blot analysis, it recognized a band at the expected molecular weight exclusively in the *FLAG*_Pb14-3-3 transgenic line (supplemental Fig. S2*A*).

14-3-3 proteins have been described as multitask proteins able to establish interactions with a broad range of molecules in a phosphorylation-dependent fashion. To verify whether this holds true for the *Plasmodium* protein, FLAG-specific mAbs were used to immunoprecipitate FLAG-Pb14-3-3 from sonicated transgenic parasite extracts. A control immunoprecipitation from the parental HP strain was performed. The recombinant GST-Pb14-3-3 was then used in an overlay assay on blotted immunoprecipitation material. The recombinant probe displayed a complex pattern of interactions with the immunoprecipitation from the transgenic *FLAG*_Pb14-3-3 line, whereas no interaction with the control material was detected (supplemental Fig. S2*B*). In the presence of the competing A8Ap phosphopeptide or using phosphatase-treated immunoprecipitation material, the interactions were significantly hampered, confirming the specificity and the phosphorylation-dependent binding of Pb14-3-3 (supplemental Fig. S2*C*).

Erythroid Dematin Is Complexed in Vivo with Pb14-3-3—A small scale proteomic analysis was performed using MALDI MS to identify proteins interacting with the FLAG-tagged 14-3-3. Intriguingly, host dematin (or erythrocyte band 4.9) was detected among the proteins co-immunoprecipitated along with the FLAG-Pb14-3-3 from the transgenic line but not in control immunoprecipitation from isogenic, parental *P. berghei*. Dematin is an actin-binding and -bundling protein present as a trimer of two 48-kDa subunits and one 52-kDa subunit at the spectrin-actin junction of the erythrocyte membrane skeleton. The 52-kDa dematin differs from the 48-kDa isoform only for the insertion of an P-loop ATP-binding site at the C-terminal portion.

The 48- and 52-kDa isoforms (accession numbers Q9WVM2 and Q9WV69, respectively) were both compatible with the 13 peptides detected by our MS analysis and covered, respectively, 44 and 40% of the two isoforms (supplemental Fig. S2*D*). An accurate search in the PlasmoDB data base did not retrieve orthologs of dematin in *Plasmodium* genomes.

The interaction between host dematin and Pb14-3-3 was verified by pulldown and co-immunoprecipitation experiments. Glutathione-Sepharose-immobilized GST-Pb14-3-3 or GST as a control was incubated with a *P. berghei* extract solubilized by sonication. The eluted proteins were subjected to Western blot analysis using an α-dematin mAb. A doublet band at 48 and 52 kDa, compatible with the size of the two dematin isoforms, and a lower band, most probably due to partial proteolytic degradation of dematin, were detected only in the GST-Pb14-3-3 sample (Fig. 2*A*).

The α-dematin mAb was able to co-immunoprecipitate the two isoforms of the protein and the Pb14-3-3 from parasite extracts (Fig. 2*B*). A direct interaction between *Plasmodium* 14-3-3 and host dematin was suggested by overlay experi-

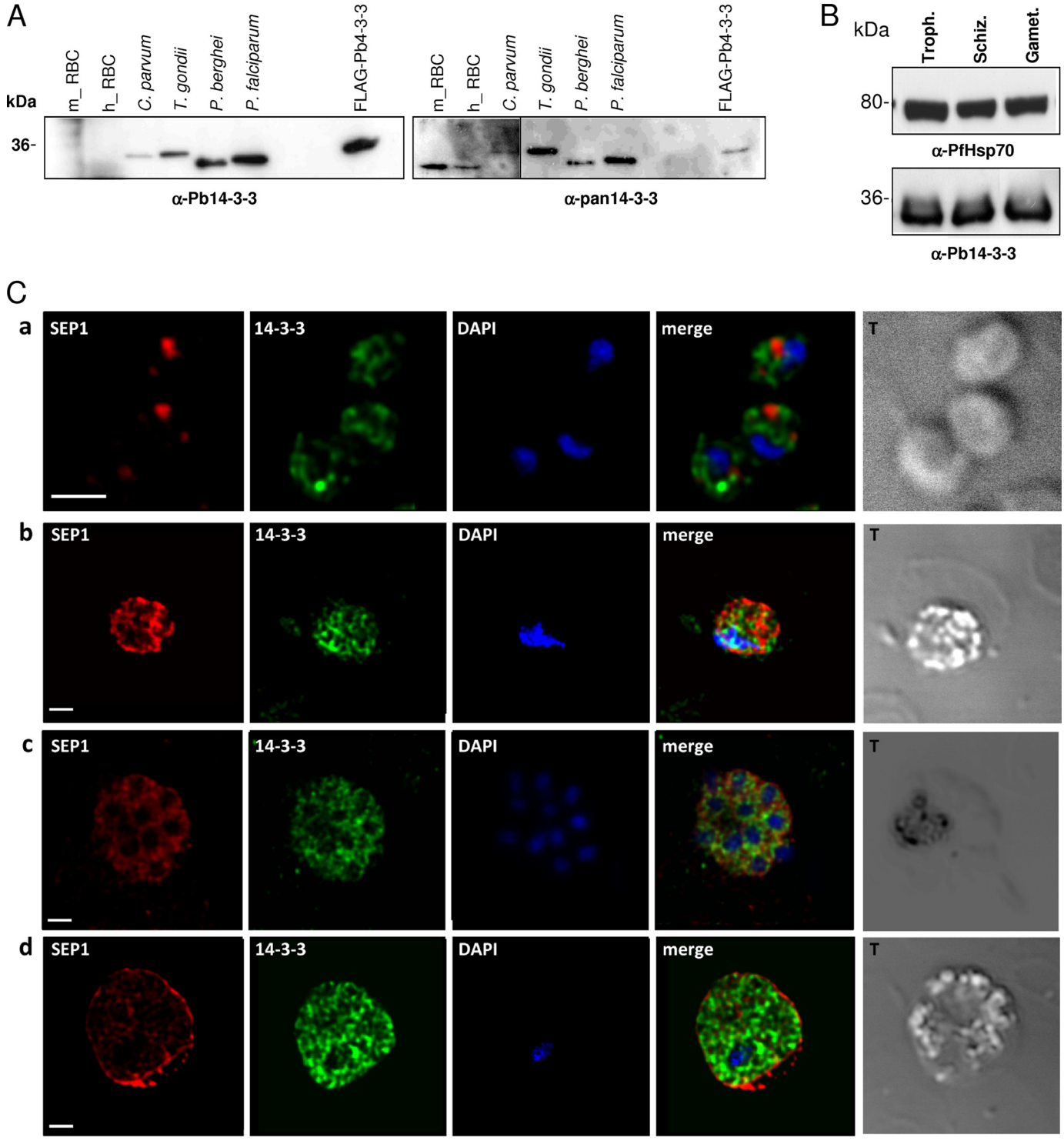

FIGURE 1. **Expression and localization of Pb14-3-3 protein.** *A*, equal amounts of protein extracts from mouse (*m*) and human (*h*) RBCs, *T. gondii* tachyzoites, *C. parvum* sporozoites, and asynchronous *P. falciparum* and *P. berghei* parasites were blotted and sequentially probed with mouse α-Pb14-3-3 serum and rabbit α-pan 14-3-3 polyclonal Abs. 1 μg of recombinant Pb14-3-3 (FLAG-Pb14-3-3) was used as a control. Two different exposures of α-pan 14-3-3 are presented. *B*, soluble proteins from *P. berghei* trophozoite (*Troph.*), schizont (*Schiz.*), and gametocyte (*Gamet.*) stages were blotted and sequentially probed with α-Pb14-3-3 and α-PfHsp70 immune sera. *C*, CLSM observations of mouse erythrocytes infected by *P. berghei* at different developmental stages: free merozoite (*panel a*), trophozoite (*panel b*), schizont (*panel c*), and gametocyte (*panel d*), stained with α-SEP1 (*red*) and α-Pb14-3-3 (*green*). Nuclei are stained with DAPI (*blue*). Displayed micrographs correspond to a single stack encompassing the center of the nucleus. *T*, transmission light acquisition. *Scale bars*, 1 μm.

ments on the immunoprecipitation (Fig. 2*B*, *third panel*). Binding specificity in the overlay assay was confirmed by inhibiting the interaction through the addition of the A8Ap phosphopeptide (Fig. 2*B*, *fourth panel*).

Host Dematin Is Recruited by Plasmodium Parasite—We showed above that Pb14-3-3 is confined within the PVM, whereas host dematin has been extensively characterized as a component of the erythrocyte membrane skeleton in normal

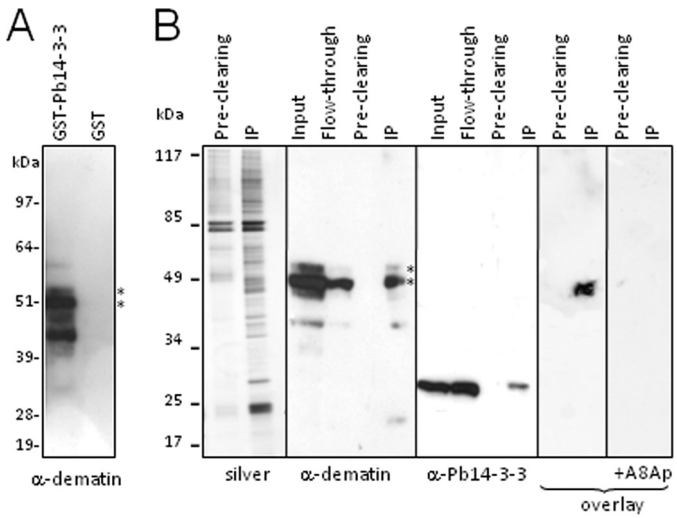

FIGURE 2. **Erythroid dematin directly interacts with Pb14-3-3.** *A*, glutathione-Sepharose-immobilized GST-Pb14-3-3 or GST as a control was incubated with a *P. berghei* extract solubilized by sonication. The eluted proteins were subjected to Western blot analysis using an α-dematin mAb. *B*, dematin was immunopurified from *P. berghei* parasites using the specific α-dematin mAb. Parasite extract (input, 1/100), pretreated with protein-G beads (preclearing, 1/20), was incubated with α-dematin-conjugated protein-G beads. After removal of the unbound material (flow-through, 1/100), immunoprecipitated proteins were eluted (*IP*, 1/20). Blotted samples were probed with α-dematin mAb and α-Pb14-3-3. The overlay assay was performed using GST-Pb14-3-3 as a probe. The interactions were inhibited through the addition of the A8Ap phosphopeptide. *Asterisks* in both panels indicate the bands corresponding to the 48- and 52-kDa dematin.

RBCs. It is then crucial to define the subcellular localization of dematin in the iRBCs to verify whether and where it might come into contact with Pb14-3-3 *in vivo*. To this aim, we analyzed the subcellular localization of dematin by CLSM in normal and infected RBCs using the α-dematin mAb and an antiserum against the PVM marker SEP1. As shown in micrographs corresponding to single z-stacks (Fig. 3*A*), dematin-specific fluorescence decorated normal and *P. berghei*-infected RBCs with a punctate pattern. In iRBCs, dematin was also detected inside the parasite and possibly at the parasitophorous vacuole, as shown by partial co-localization with PbSEP1.

In Western blot analyses of fractionated extracts from enriched asexual and sexual *P. berghei* blood stages (Fig. 3*B*), the α-dematin mAb detected a doublet at 48 and 52 kDa, mainly in the insoluble material after high salt extraction. The same bands were also revealed in RBC ghosts. In these samples, Pb14-3-3 was detected in both soluble and insoluble fractions from parasite blood stages but not RBC ghosts. Dematin, present in parasite extracts, was also resistant to extraction with non-ionic detergents such as Triton X-100 (data not shown), whereas a nearly complete solubilization of both dematin and 14-3-3 was obtained by sonication (Fig. 3*C*), the procedure adopted in the immunoprecipitation experiments.

Although the α-dematin mAb used in this study detected the expected bands in Western blot analysis, the fluorescence intensity observed by CLSM appeared to be higher inside the parasite than at the periphery of the iRBC (Fig. 3*A*, *panel a*). This apparent discrepancy might be explained by a different accessibility of the parasite-recruited dematin to the mAb. To confirm that dematin is partly recruited inside the parasite, a polyclonal mouse immune serum against a recombinant 52-kDa mouse dematin (m52kd) was prepared.

The m52kd serum detected the expected protein bands at 48 and 52 kDa in fractionated *P. berghei* protein extracts as well as in mouse RBC ghosts (supplemental Fig. S3*A*). In CLSM analysis of *P. berghei* iRBC, the m52kd serum clearly detected a strong dematin-specific signal inside the parasite and at the surface of infected and normal RBCs (supplemental Fig. S3*B*), thus confirming the results obtained with the α-dematin mAb. We then extended the analysis to human erythrocytes infected by *P. falciparum* to establish whether the recruitment of dematin is a conserved aspect in the host/parasite interplay.

Fractionated *P. falciparum* iRBCs were subjected to Western blot analysis. As shown (Fig. 4*A*), α-Pb14-3-3 detected *P. falciparum* 14-3-3 in the parasite pellet after iRBC lysis as well as in Triton-soluble and insoluble parasite fractions but not in ghosts prepared from iRBC supernatant. Conversely, an antibody specific for human 14-3-3 isoforms detected the proteins in iRBC ghosts but not in the parasite fractions. As expected, dematin was detected in both ghost and parasite preparations. As in the case of *P. berghei*, internalized dematin was mainly recovered in Triton-insoluble parasite fractions.

Immunolocalization of dematin in *P. falciparum* blood stages was performed in combination with anti-EXP1 that specifically stains a PVM resident protein. CLSM analysis (Fig. 4*B*) showed a dematin staining profile largely comparable with that observed in *P. berghei* blood stages, with dematin recruited into the parasite and partially at the PVM, as confirmed by co-staining with EXP1. A punctate labeling of the cell membrane was visible in normal and infected RBCs.

To confirm dematin internalization, we treated *P. falciparum* iRBCs and normal RBCs with streptolysin-O (23, 26), following a well established procedure for selectively permeabilizing human RBC membranes, and subjected them to proteinase K (PK) digestion. The treated samples were then probed with specific immune sera (Fig. 4*C*). In both infected and uninfected ghosts, dematin was accessible to PK digestion. In the parasite fraction, it was instead protected from protease digestion, indicating that dematin is entirely internalized. The effectiveness of PK digestion was confirmed using the α-BR5 immune serum (18) against the *P. falciparum* Maurer's cleft transmembrane protein Pfsbp1 (48 kDa in size). α-BR5 recognizes the N-terminal portion of the protein localized within the lumen of the organelle. Following PK digestion, α-BR5 reacts with a 37-kDa polypeptide generated by the proteolytic digestion of the C-terminal domain facing the host cell cytoplasm. As shown in Fig. 4*C*, the α-BR5 antiserum detected exclusively the 37-kDa digestion product in the treated sample, indicating that both streptolysin-O permeabilization and PK digestion were effective.

Dematin-Pb14-3-3 Interaction Is Promoted by cAMP-dependent Phosphorylation—14-3-3 binding occurs generally on well defined serine- or threonine-phosphorylated motifs present in the target molecule (12). These motifs partially overlap sequences phosphorylated by the PKA and the casein kinases I and II (12).

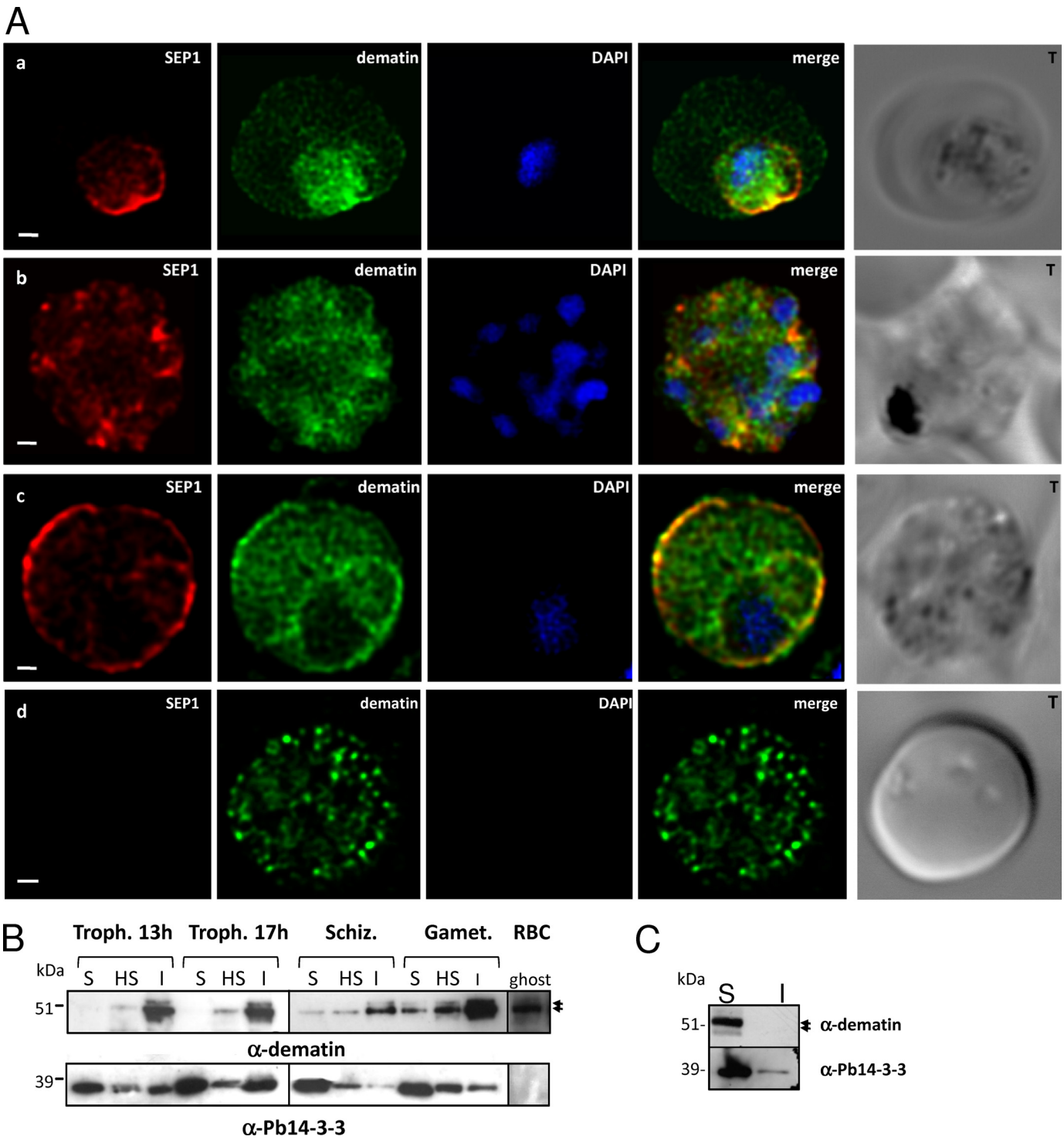

FIGURE 3. **Subcellular localization of dematin in *P. berghei*-infected mouse RBC.** *A*, CLSM observations of mouse erythrocytes infected by *P. berghei* at different developmental stages: trophozoite (*panel a*), schizont (*panel b*), gametocyte (*panel c*), and a normal RBC (*panel d*), stained with α-SEP1 (*red*) and α-dematin mAb (*green*). Nuclei were stained with DAPI (*blue*). Displayed micrographs correspond to the single stack encompassing the center of the parasite nucleus. *T*, transmission light acquisition. *Scale bars*, 0.5 μm. *B*, soluble (*S*), high salt soluble (*HS*), and insoluble (*I*) proteins from *P. berghei* young (*Troph. 13h*) and late (*Troph. 17h*) trophozoites, schizonts (*Schiz.*), gametocytes (*Gamet.*) and total ghost proteins from normal mouse RBCs were blotted and sequentially probed with α-Pb14-3-3 and α-dematin mAb. *Arrows* indicate the 48–52-kDa dematin doublet. *C*, *P. berghei* soluble (*S*) and insoluble (*I*) proteins obtained by sonication were blotted and sequentially probed with α-Pb14-3-3 and α-dematin mAb. *Scale bars*, 1 μm.

Phosphorylation of dematin by different protein kinases, including PKA, has been described in mammalian erythrocytes (27, 28). To explore the involvement of PKA in promoting dematin-14-3-3 interactions, a recombinant, GST-fused 52-kDa isoform of dematin was phosphorylated *in vitro* using the PKA catalytic subunit or casein kinase II. The recombinant dematin was phosphorylated by PKA but not by casein kinase II (Fig. 5*A*).

The ability of PKA-phosphorylated dematin to bind Pb14-3-3 was then tested in pulldown experiments using a bacterial

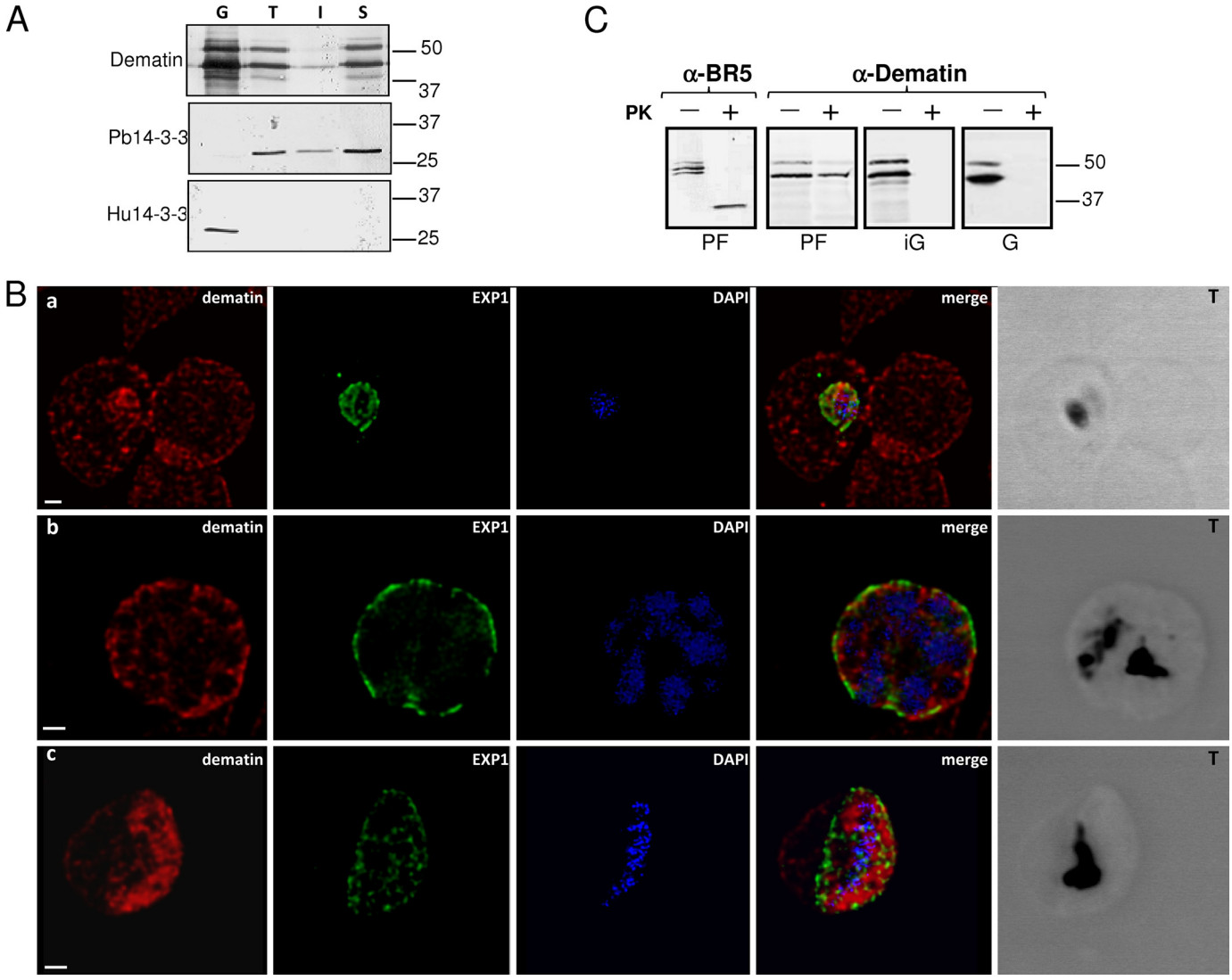

FIGURE 4. **Localization of dematin in *P. falciparum* iRBC.** *A*, ghosts (*G*) and parasite-enriched fraction (*T*) were separated from iRBCs. Parasite fraction was treated with Triton X-100 to obtain soluble (*S*) and insoluble (*I*) proteins. Blotted samples were probed with α-dematin mAb, α-Pb14-3-3, and α-Hu14-3-3γ serum (specific for the human 14-3-3 isoforms). *B*, CLSM observations of normal human RBCs (*panel a*) and erythrocytes infected by *P. falciparum* at different developmental stages: trophozoite (*panel a*), schizont (*panel b*), and gametocyte (*panel c*), stained with the α-EXP1 serum (*green*), which decorates the PVM, and the α-dematin md52k serum (*red*). Nuclei were stained with DAPI (*blue*). Displayed micrographs correspond to a single stack encompassing the center of the nucleus. *T*, transmission light acquisition. *Scale bars*, 1 μm. *C*, parasite fraction (*PF*) and ghosts from iRBC (*iG*) or normal RBC (*G*) were treated with streptolysin-O and incubated (+) or not (−) with PK, blotted, and probed with α-dematin mAb. The effectiveness of PK treatment was confirmed using the α-BR5 immune serum against the *P. falciparum* Maurer's cleft transmembrane protein Pfsbp1. In the PK-treated sample, α-BR5 reacts with a 37-kDa polypeptide.

lysate containing a His-tagged Pb14-3-3. Proteins bound to GST-dematin beads were first eluted with the A8Ap phosphopeptide and then with glutathione. The eluted material was probed using an anti-His antibody. As shown in Fig. 5*B*, His-Pb14-3-3 bound exclusively the phosphorylated GST-dematin.

Multiple putative 14-3-3-binding sites were identified by scanning the 52-kDa isoform of dematin, using the Minimotif Miner application and the Eukaryotic Linear Motif (ELM) resource (Fig. 5*C*). The sequences ^{122}RTSLP^{126}, ^{330}RGNSLP^{335}, and ^{399}KKASLF^{405}, reproducing, respectively, mode-1, mode-2, and a C-terminal mode-3-like binding motif (25, 29), were selected for further analysis. In particular, Ser^{333} and Ser^{403} were previously described as *in vivo* phosphorylated residues (4, 30, 31). Single, double, and triple point mutants of 52-kDa dematin were generated at the selected sites and phosphorylated *in vitro* by PKA. As shown in Fig. 5*D*, radioactive phosphate was incorporated into wild type dematin and the mutant forms at comparable levels, except for the triple mutant S124A/S333A/S403A, where signal intensity was slightly reduced. This result suggests that PKA-phosphorylatable sites other than those examined here are present in 52-kDa dematin. In pulldown experiments, the Pb14-3-3-dematin interaction was affected in Ser^{124} and Ser^{333} single or double mutants (Fig. 5*E*), suggesting that both sites might be required for optimal Pb14-3-3 binding.

DISCUSSION

This study is the first report showing that the actin-binding and -bundling protein dematin, a component of the erythro-

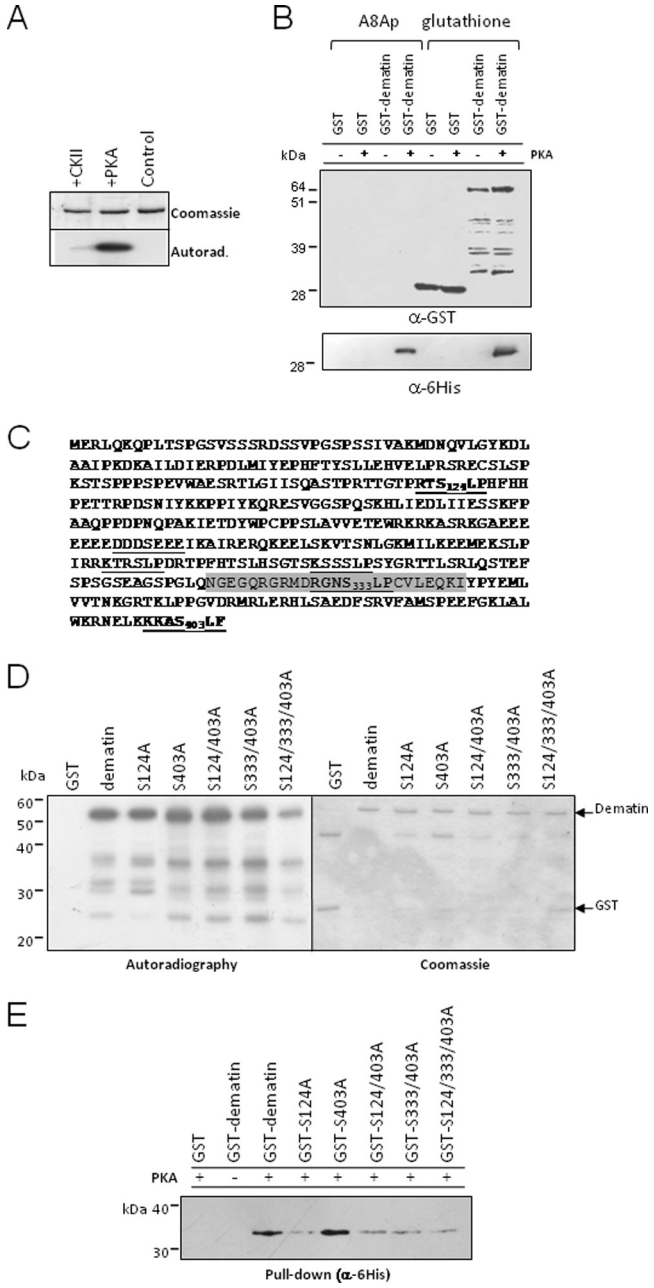

FIGURE 5. **Dematin-Pb14-3-3 interaction is promoted by PKA phosphorylation.** *A*, a GST-fused 52-kDa isoform of dematin was phosphorylated *in vitro* using the PKA catalytic subunit or casein kinase II (*CKII*), digested with the PreScission enzyme, and run in SDS-PAGE. A control sample without enzymes was also included. Autoradiography (*Autorad.*) of the stained gel showed that the recombinant dematin was efficiently labeled only by PKA. *B*, glutathione-Sepharose-immobilized GST or GST-dematin, phosphorylated (+) or not (−) with PKA, was incubated with a bacterial lysate containing His-Pb14-3-3. Proteins eluted with A8Ap synthetic phosphopeptide or glutathione were blotted and probed with α-His_6, to detect the associated 14-3-3, or α-GST, to detect the eluted recombinant GST and GST-dematin. *C*, putative 14-3-3-binding sites on the 52-kDa dematin isoform are *underlined*. Putative PKA phosphorylation sites coinciding with the 14-3-3-binding sites are in *bold*. The position of mutated serines is specified. The ATP-binding site (P-loop) is *boxed* in *gray*. *D*, recombinant GST, GST-dematin, or GST-dematin mutants, bound to glutathione-Sepharose beads, were phosphorylated by the PKA catalytic subunit. Phosphorylated recombinant proteins, digested with the PreScission enzyme, were run in SDS-PAGE, stained with Coomassie Blue, and subjected to autoradiography. *E*, GST, GST-dematin, and GST-dematin mutants were treated as in *panel B*. Proteins eluted from the glutathione-Sepharose beads with the A8Ap synthetic phosphopeptide were subjected to immunoblotting using the α-His_6 to detect bound 14-3-3.

cyte spectrin-based membrane skeleton, is recruited by the malaria parasite following erythrocyte infection. Internalized dematin is able to establish an unexpected interaction with the *Plasmodium* regulatory protein 14-3-3. We have shown that *Plasmodium* 14-3-3 does not exit from the parasite. Thus, it might determine the localization of dematin inside the parasite but not its displacement from the junctional complex and subsequent transport across the erythrocyte cytoplasm.

Dematin and parasite 14-3-3 directly interact both *in vivo* and *in vitro*. Their interaction, at least *in vitro*, is strictly dependent on dematin phosphorylation, here effected by PKA, mainly at the Ser^{124} and Ser^{333} residues, which belong to two putative 14-3-3-binding motifs, ^{122}RTSLP^{126} and ^{330}RGNSLP^{335}. Previous observations suggested a role of PKA in the development of parasite blood stages. The level of cAMP increases in *P. falciparum*-infected erythrocytes (32) and, consistently, the use of a host-specific PKA inhibitor greatly affects parasite development (33, 34). It is well documented that dematin is a substrate for multiple protein kinases, including PKA and PKC, both *in vivo* and *in vitro*, and that its interactions with spectrin, actin, and the plasma membrane are regulated by its phosphorylation status (4, 30). Phosphorylated forms of dematin were also purified from liver and synapses (31, 35). It is conceivable that variations in the phosphorylation status of dematin, as a consequence of parasite invasion, may cause a partial displacement of this protein, thus favoring its mobilization and recruitment by the parasite.

It has been shown that in mice expressing a headpiece domain-deleted form of dematin, erythrocyte shape and membrane stability are affected (36–38). Hence, it is conceivable that the repositioning of dematin that follows parasite infection might determine a temporary instability of the spectrin-actin skeleton and membrane cohesion, thus providing opportunities for new interactions with parasite proteins. A number of *P. falciparum* proteins were, in fact, described to bring about coordinated remodeling of the erythrocyte membrane skeleton (3, 9). For example, the ring-infected erythrocyte surface antigen (RESA), one of the first parasite proteins routed to the RBC skeleton, binds and stabilizes spectrin.

Hereditary defects of the RBC membrane skeleton have been related to malaria resistance. *In vitro* studies on the ability of *P. falciparum* to invade RBCs from patients with hereditary ovalocytosis, associated with mutation on band 3 protein, or elliptocytosis, caused by spectrin self-association defects or deficiency of protein 4.1, resulted in a reduction in parasitic invasion. Such reduction is more significant from the second invasion cycle (39–41). Impaired recruitment of host skeletal proteins might explain a progressively diminishing ability of the malaria parasite to invade defective RBCs.

In conclusion, we propose that the coordinated remodeling of the erythrocyte skeleton involves not only the binding of parasite proteins to the cytoskeleton but also the mobilization of resident components of the host junctional complex and their recruitment by the parasite. The erythrocyte is a terminally differentiated, anucleated cell with a few, very specialized functions. This led to the current view that *Plasmodium*

molecules are the only active actors in host-parasite interactions. Recent data demonstrate that host cell molecules are of crucial importance for key steps of parasite development. Erythrocyte calpain-1 is required *in vitro* for parasite egress from the infected erythrocyte (42), whereas *de novo* polymerization of host actin occurs during entry of *T. gondii* tachyzoites and *P. berghei* sporozoites (43). Understanding the role of key erythrocyte molecules may help design strategies that prevent a cascade of events leading to host cell remodeling and/or parasite development during malaria infection.

Acknowledgments—We thank Dr. Tamara Petrucci and Dr. Marco Crescenzi for the critical reading of the manuscript, Dr. Cecilia Birago for fruitful discussion, Dr. Prisca Boisguerin for pepscan design and Leonardo Picci for technical assistance, and Dr. Furio Spano and Dr. Fabio Tosini, respectively, for the kindly gift of the T. gondii tachyzoites of the strains RH and C. parvum oocysts.

REFERENCES

1. Marti, M., Good, R. T., Rug, M., Knuepfer, E., and Cowman, A. F. (2004) *Science* **306,** 1930–1933
2. Hiller, N. L., Bhattacharjee, S., van Ooij, C., Liolios, K., Harrison, T., Lopez-Estraño, C., and Haldar, K. (2004) *Science* **306,** 1934–1937
3. Maier, A. G., Cooke, B. M., Cowman, A. F., and Tilley, L. (2009) *Nat. Rev. Microbiol.* **7,** 341–354
4. Azim, A. C., Knoll, J. H., Beggs, A. H., and Chishti, A. H. (1995) *J. Biol. Chem.* **270,** 17407–17413
5. Bruce, L. J., Beckmann, R., Ribeiro, M. L., Peters, L. L., Chasis, J. A., Delaunay, J., Mohandas, N., Anstee, D. J., and Tanner, M. J. (2003) *Blood* **101,** 4180–4188
6. Marfatia, S. M., Lue, R. A., Branton, D., and Chishti, A. H. (1994) *J. Biol. Chem.* **269,** 8631–8634
7. Khan, A. A., Hanada, T., Mohseni, M., Jeong, J. J., Zeng, L., Gaetani, M., Li, D., Reed, B. C., Speicher, D. W., and Chishti, A. H. (2008) *J. Biol. Chem.* **283,** 14600–14609
8. Anong, W. A., Franco, T., Chu, H., Weis, T. L., Devlin, E. E., Bodine, D. M., An, X., Mohandas, N., and Low, P. S. (2009) *Blood* **114,** 1904–1912
9. Maier, A. G., Rug, M., O'Neill, M. T., Brown, M., Chakravorty, S., Szestak, T., Chesson, J., Wu, Y., Hughes, K., Coppel, R. L., Newbold, C., Beeson, J. G., Craig, A., Crabb, B. S., and Cowman, A. F. (2008) *Cell* **134,** 48–61
10. Di Girolamo, F., Raggi, C., Birago, C., Pizzi, E., Lalle, M., Picci, L., Pace, T., Bachi, A., de Jong, J., Janse, C. J., Waters, A. P., Sargiacomo, M., and Ponzi, M. (2008) *Proteomics* **8,** 2500–2513
11. Al-Khedery, B., Barnwell, J. W., and Galinski, M. R. (1999) *Mol. Biochem. Parasitol.* **102,** 117–130
12. Aitken, A. (2006) *Semin. Cancer Biol.* **16,** 162–172
13. Janse, C. J., and Waters, A. P. (1995) *Parasitol. Today* **11,** 138–143
14. Janse, C. J., Franke-Fayard, B., Mair, G. R., Ramesar, J., Thiel, C., Engelmann, S., Matuschewski, K., van Gemert, G. J., Sauerwein, R. W., and Waters, A. P. (2006) *Mol. Biochem. Parasitol.* **145,** 60–70
15. Trager, W., and Jensen, J. B. (1976) *Science* **193,** 673–675
16. Lalle, M., Salzano, A. M., Crescenzi, M., and Pozio, E. (2006) *J. Biol. Chem.* **281,** 5137–5148
17. Trasarti, E., Pizzi, E., Pozio, E., and Tosini, F. (2007) *Mol. Biochem. Parasitol.* **152,** 159–169
18. Blisnick, T., Morales Betoulle, M. E., Barale, J. C., Uzureau, P., Berry, L., Desroses, S., Fujioka, H., Mattei, D., and Braun Breton, C. (2000) *Mol. Biochem. Parasitol.* **111,** 107–121
19. Dat, M. H., Behr, C., Jouin, H., Baleux, F., Mercereau-Puijalon, O., and Dubois, P. (2000) *Parasite Immunol.* **22,** 535–543
20. Birago, C., Albanesi, V., Silvestrini, F., Picci, L., Pizzi, E., Alano, P., Pace, T., and Ponzi, M. (2003) *Mol. Biochem. Parasitol.* **126,** 209–218
21. Behari, R., and Haldar, K. (1994) *Exp. Parasitol.* **79,** 250–259
22. Pozuelo Rubio, M., Peggie, M., Wong, B. H., Morrice, N., and MacKintosh, C. (2003) *EMBO J.* **22,** 3514–3523
23. Jackson, K. E., Spielmann, T., Hanssen, E., Adisa, A., Separovic, F., Dixon, M. W., Trenholme, K. R., Hawthorne, P. L., Gardiner, D. L., Gilberger, T., and Tilley, L. (2007) *Biochem. J.* **403,** 167–175
24. Petosa, C., Masters, S. C., Bankston, L. A., Pohl, J., Wang, B., Fu, H., and Liddington, R. C. (1998) *J. Biol. Chem.* **273,** 16305–16310
25. Yaffe, M. B., Rittinger, K., Volinia, S., Caron, P. R., Aitken, A., Leffers, H., Gamblin, S. J., Smerdon, S. J., and Cantley, L. C. (1997) *Cell* **91,** 961–971
26. Ansorge, I., Benting, J., Bhakdi, S., and Lingelbach, K. (1996) *Biochem. J.* **315,** 307–314
27. Hosey, M. M., and Tao, M. (1976) *Biochemistry* **15,** 1561–1568
28. Plut, D. A., Hosey, M. M., and Tao, M. (1978) *Eur. J. Biochem.* **82,** 333–337
29. Coblitz, B., Shikano, S., Wu, M., Gabelli, S. B., Cockrell, L. M., Spieker, M., Hanyu, Y., Fu, H., Amzel, L. M., and Li, M. (2005) *J. Biol. Chem.* **280,** 36263–36272
30. Husain-Chishti, A., Levin, A., and Branton, D. (1988) *Nature* **334,** 718–721
31. Collins, M. O., Yu, L., Coba, M. P., Husi, H., Campuzano, I., Blackstock, W. P., Choudhary, J. S., and Grant, S. G. (2005) *J. Biol. Chem.* **280,** 5972–5982
32. Read, L. K., and Mikkelsen, R. B. (1991) *Mol. Biochem. Parasitol.* **45,** 109–119
33. Syin, C., Parzy, D., Traincard, F., Boccaccio, I., Joshi, M. B., Lin, D. T., Yang, X. M., Assemat, K., Doerig, C., and Langsley, G. (2001) *Eur. J. Biochem.* **268,** 4842–4849
34. Sudo, A., Kato, K., Kobayashi, K., Tohya, Y., and Akashi, H. (2008) *Mol. Biochem. Parasitol.* **160,** 138–142
35. Villén, J., Beausoleil, S. A., Gerber, S. A., and Gygi, S. P. (2007) *Proc. Natl. Acad. Sci. U.S.A.* **104,** 1488–1493
36. Gilligan, D. M., Lozovatsky, L., Gwynn, B., Brugnara, C., Mohandas, N., and Peters, L. L. (1999) *Proc. Natl. Acad. Sci. U.S.A.* **96,** 10717–10722
37. Muro, A. F., Marro, M. L., Gajović, S., Porro, F., Luzzatto, L., and Baralle, F. E. (2000) *Blood* **95,** 3978–3985
38. Khanna, R., Chang, S. H., Andrabi, S., Azam, M., Kim, A., Rivera, A., Brugnara, C., Low, P. S., Liu, S. C., and Chishti, A. H. (2002) *Proc. Natl. Acad. Sci. U.S.A.* **99,** 6637–6642
39. Chishti, A. H., Palek, J., Fisher, D., Maalouf, G. J., and Liu, S. C. (1996) *Blood* **87,** 3462–3469
40. Cortés, A., Benet, A., Cooke, B. M., Barnwell, J. W., and Reeder, J. C. (2004) *Blood* **104,** 2961–2966
41. Dhermy, D., Schrével, J., and Lecomte, M. C. (2007) *Curr. Opin. Hematol.* **14,** 198–202
42. Chandramohanadas, R., Davis, P. H., Beiting, D. P., Harbut, M. B., Darling, C., Velmourougane, G., Lee, M. Y., Greer, P. A., Roos, D. S., and Greenbaum, D. C. (2009) *Science* **324,** 794–797
43. Gonzalez, V., Combe, A., David, V., Malmquist, N. A., Delorme, V., Leroy, C., Blazquez, S., Ménard, R., and Tardieux, I. (2009) *Cell. Host Microbe* **5,** 259–272